Heliyon 8 (2022) e08903

Contents lists available at ScienceDirect

Heliyon

journal homepage: www.cell.com/heliyon

Research article

Prediction of electronic properties of novel ZnS–ZnO-recycled expanded polystyrene nanocomposites by DFT

Rokhsareh Akbarzadeh [a,**], Olusola Olaitan Ayeler [b], Qusai Ibrahim [c], Peter Apata Olubambi [b], Patrick Ndungu [a,*]

[a] Energy, Sensors and Multifunctional Nanomaterials Research Group, Department of Chemical Sciences, Faculty of Science, University of Johannesburg, Doornfontein, 2028, South Africa
[b] Centre for Nanoengineering and Tribocorrosion (CNT), University of Johannesburg, Johannesburg, 2028, South Africa
[c] School of Engineering and Design, Institute of Technology Sligo, Ash Lane, Sligo, Ireland

GRAPHICAL ABSTRACT

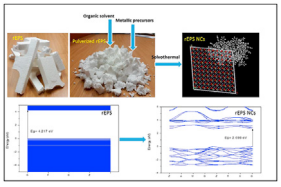

ARTICLE INFO

Keywords:
Recycled expanded polystyrene
Density functional theory
ZnO
ZnS
Electronic structure

ABSTRACT

DFT calculations using Material Studio (2019) were used to ascertain the changes in electronic properties of recycled expanded polystyrene (rEPS) after modification with nanoparticles of ZnS and ZnO. The nanocomposites were obtained using rEPS and suitable metal salt precursors via a solvothermal method. The XRD analysis was conducted to obtain the crystallography data of the new rEPS-based nanocomposites. Using Material Studio simulation software, the potential photocatalytic properties of the new prepared material was predicted and information on the electronic band structure was extracted. The calculated band gap values for rEPS and ZnS–ZnO-rEPS nanocomposite were 4.217 eV and 2.698 eV, respectively. Furthermore, our results showed that the nanocomposite is a p-type semiconductor. From the electronic structure and the band gap narrowing, these nanocomposites obtained from a waste material may have some potential in photocatalytic applications.

1. Introduction

In general, rapid population growth, increased urbanization, industrialization and continual economic growth have been major contributing factors to the increase in the amount of generated municipal solid waste in developing countries, and around the world [1]. Municipal solid waste is generated from various anthropogenic activities, and has been linked to several health issues experienced by members of the public, and degradation of the local environment [2, 3]. Many nations around the world are now faced with diverse problems arising from poor municipal solid waste management; one particular problem is due to modern reliance and use of certain types of polymeric materials, which on disposal then eventually become waste plastics. Plastics, as a waste material has continued to grow in the general biosphere and several efforts have been made to reduce the impact of plastic waste in the environment because of the health and environmental implications. Some recent research trends

* Corresponding author.
** Corresponding author.
E-mail addresses: rakbarzadeh@uj.ac.za (R. Akbarzadeh), pndungu@uj.ac.za (P. Ndungu).

https://doi.org/10.1016/j.heliyon.2022.e08903
Received 25 September 2020; Received in revised form 14 November 2020; Accepted 1 February 2022

in the open literature have shown a growing interest in combining inorganic metallic precursors with recycled plastics to form nanocomposites. Such nanocomposites can have various improved properties when matched appropriately with the primary material [4, 5]. Thus, fundamental research to create novel nanocomposites with better physical-chemical properties, and at the same time mitigate some of the challenges associated with waste management, can provide new strategies to reduce the harmful impact to public health and help improve and protect the natural environment [6, 7, 8].

Polymer nanocomposites can have semi-conductive properties when combining polymers with semiconducting materials [9]. Nanoparticles have been used as a filler for the enhancement of the physical-chemical properties of polymeric materials. Some examples include SiO_2, Al_2O_3, TiO_2, and ZnO nanoparticles, either as reinforcement materials, or as a means to improve the optical or photo-catalytic properties [10, 11]. Alternatively, polymers can be processed into nano-particulate forms and used in a wide range of applications; such as nanoreactors, coating materials, electrochemical biosensors, drug delivery, nanocarriers, catalysts and polymer composite fabrication [12]. In terms of some early reports on the application of nanoparticle-polymer composites, a titania iron oxide photo-catalysts supported on polyethylene was used as an effective material for degradation of resorcinol [13]. The interest in such early work highlights the potential to investigate the use of recycled expanded polystyrene (rEPS) as a catalyst support, and furthering efforts to convert waste materials to value added material. Prior or parallel to any experimental work that can explore the potential of a semiconductor nanoparticle-polymer nanocomposites as a photocatalyst, computational simulation studies can provide some valuable insights. Researchers have carried out studies on electronic and other properties using computer simulation methods. Computer simulation methods, also known as computer experiments, can complement experimental work in the laboratory and as such serve as a bridge between laboratory experiments and theoretical calculations [14]. Based on the relevant information available in the open literature, studies that analyse the electronic properties of polymer composites and their photocatalytic performances are very limited. In this work, DFT calculations were used to analyse the effect of ZnO, and ZnS on the rEPS NCs nanocomposite's electronic properties and to predict its semiconducting properties.

2. Experimental

2.1. Synthesis

The rEPS was obtained from a recycling facility in Johannesburg, South Africa and was used in the development of the nanocomposites. The nanocomposites were synthesized as per the methods reported in our previous study by Ayeleru ***et al.*** [15]. Briefly, rEPS was crushed and then impregnated with metallic precursors, placed in an autoclave reactor, and then this was placed in an oven that had been pre-heated to 250 °C, and then heated for 3 h. The resulting products were subsequently characterized and analysed as potential photocatalytic materials.

2.2. Characterization

XRD patterns were obtained to determine the crystallographic information of the developed rEPS NCs using an X-ray diffractometer (PANalytical Empyrean) with Cu-Kα1 radiation. The crystallography information obtained from the XRD results (Table 1 and Figure 1) were then used in the simulations and DFT calculations.

2.3. Computational method

A simulation box consisting of rPES, ZnO, ZnS structures was created using Material Studio 2019 based on the experimental XRD data from this work, which are presented in Table 1 and Figure 1. The calculations were done based on first-principle theory using Cambridge serial total energy package [16]. The generalized gradient approximation (GGA) functional with the Perdew-Burke-Ernzerhof (PBE) type were used to model the exchange and correlation interactions [17]. The cut-off kinetic energy of the electron wave function ranged from 460 to 600 eV and 6 × 6 × 6 was selected as the medium quality of the k-point sampling. When the primitive cell was created, the geometry optimization task with a maximum number of 100 iterations was applied to investigate the composites lattice structure. In the geometrical optimization, the convergence of all forces on atoms were set to less than 0.05 eV/Å. The maximum stress was 0.1 GPa with the maximum displacement of 0.002Å. The band gap, density of state (DOS), and projected density of state (PDOS) were calculated by Generalized Gradient Approximation (GGA) [18], which is considered accurate with these types of calculations [19]. The considered lattice parameters and their corresponding angles are presented in Table 1.

3. Results and discussion

3.1. Structural properties

3.1.1. XRD

The XRD patterns for rEPS, ZnS–ZnO and ZnS–ZnO-rEPS nanocomposites are presented in Figure 1. The diffraction peaks for rEPS were observed at 19.8° and 10° 2θ (Figure 1), and are due to the crystalline and amorphous phases of rEPS, which agrees well with the reported data cards (JCPDS no. 33-0664). The sharp XRD peaks in ZnS–ZnO and ZnS–ZnO-rEPS nanocomposites indicate that the synthesized nanocomposites were crystalline.

The hexagonal ZnO and cubic ZnS phases were identified and the peaks agree with reference codes of JCPDS no. 01-1136, and 02-0565, respectively. In addition to the characteristic peaks of ZnO and ZnS, two broad peaks located at 19.8° and 10° 2θ were observed and these were attributed to rEPS, which confirmed the presence of rEPS in the nanocomposite. This information from the XRD data, and data from our previous work [15], were then used in building the molecular structure by simulation.

3.2. Molecular structure

In this study chains of rEPS were used as a substrate to create ZnS–ZnO-rEPS nanocomposite. Figure 2 represents the whole composite containing a total of 3054 atoms in x, y, and z coordinate system. The nanocomposite structure contains ZnO layers with 966 Zn and O atoms, and ZnS layers with 966 atoms of zinc and sulfur. This structure was set in a supercell (8 × 8 × 2 $Å^3$) and its angles were fixed at 90°.

3.3. Electronic properties

To study the electronic properties, the band gap structure and DOS are important. These two parameters give details about the electronic and optical properties of the prepared samples.

3.3.1. Band structure

The energy band structure extracted for rEPS, ZnO–ZnS and ZnS–ZnO/rEPS are shown in Figure 3 and the information have been presented in Table 2. The band gap of rEPS was 4.217eV, and the band gap of ZnS–ZnO/rEPS nanocomposite was 2.698 eV. As the band gap reduces, the chances of charge recombination increases and the smaller band gap changes the optical properties such that the material can absorb electromagnetic radiation within the UV-visible range. This reduction in the band gap, and the ability to absorb light within the UV-visible range, can consequently increase the generation of electron-hole pairs, and this potentially improves the photocatalytic activity of the nanocomposite [20, 21]. This prediction, which is based on the lattice constants obtained by experimental characterization shows that ZnS–ZnO-rEPS should have

Table 1. Lattice constants for rPES, ZnO and ZnS.

Nanocomposite		rPES	ZnO	ZnS
Lattice constants (Å)	a	21.90	3.2420	5.40
	b	21.90	3.2420	5.40
	c	6.65	5.1760	5.40
corresponding angle	α	90°	90°	90°
	β	90°	90°	90°
	γ	90°	120°	90°

better optical absorption performance than the parent polymer material. From the calculated conduction band and valence band (VB) values (Table 2), the VB values shifted to higher values (0.4459 eV) for ZnS–ZnO-rEPS. The values reported in Table 2, and the results from the simulations showed that the ZnO–ZnS sample exhibited a direct band gap similar to the reported results in previous studies [22, 23]. The ZnS–ZnO-rEPS sample, shows an indirect band gap and the calculated band gap value for the nanocomposite of rEPS with ZnO and ZnS has not been reported elsewhere. Although it has been reported that materials with direct band gaps are good for the photons absorption; however, an indirect band gap improves the life-time of the photo-generated carriers [24]. This further highlights the excellent photocatalytic potential for the nanocomposite.

3.3.2. *Density of states (DOS)*

The determination of the density of states (DOS) is another important analytic tool in investigating the electronic properties of a material. The density of states provides information on the number of electron or hole states per unit volume at a given energy level. The total density of states of rEPS and ZnS–ZnO and its composite ZnS–ZnO-rEPS are illustrated in Figure 4 (a-c). The three samples exhibit different patterns as expected, and the ZnS–ZnO-rEPS sample displays a configuration indicative of a semiconductor structure. This seems to predict an electronic structure conducive to photocatalytic applications for the ZnS–ZnO-rEPS nanocomposite, since its DOS patterns are relatively similar to the structure of

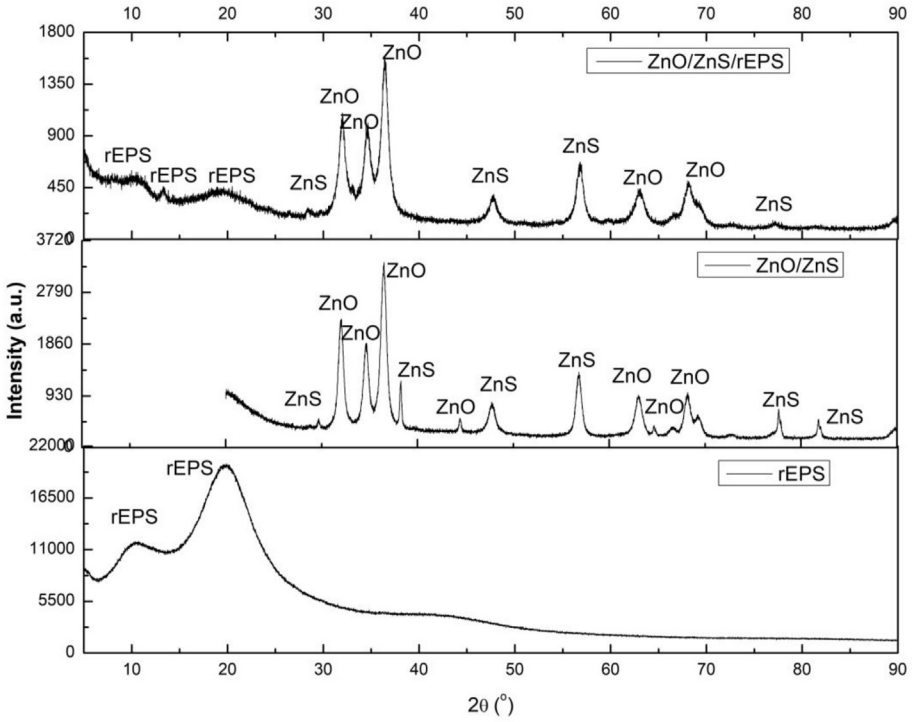

Figure 1. X-ray powder diffraction pattern for rEPS, *ZnS–ZnO* and *ZnS–ZnO-rEPS*.

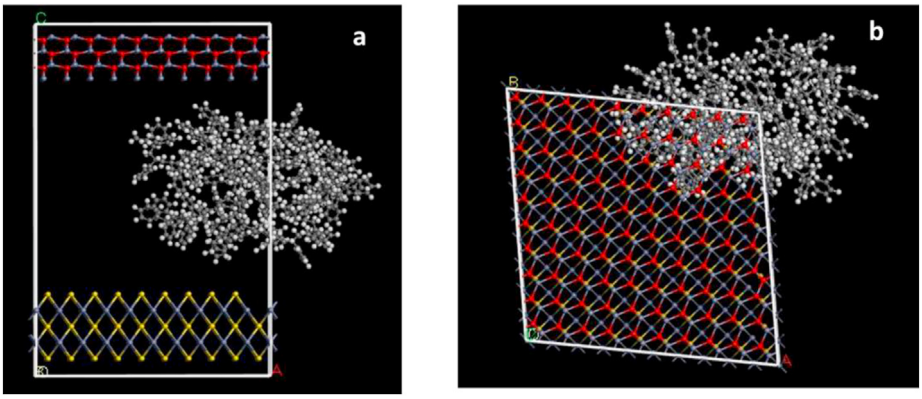

Figure 2. Molecular structure of ZnO–ZnS-rEPS nanocomposite, ZnO atoms with (Zn atoms in blue, Oxygen atoms in red), ZnS (Zn atoms in blue, Sulfide atoms in yellow), and rEPS (Carbon atoms in dark grey, and Hydrogen atoms in white). a) side view, b) top view.

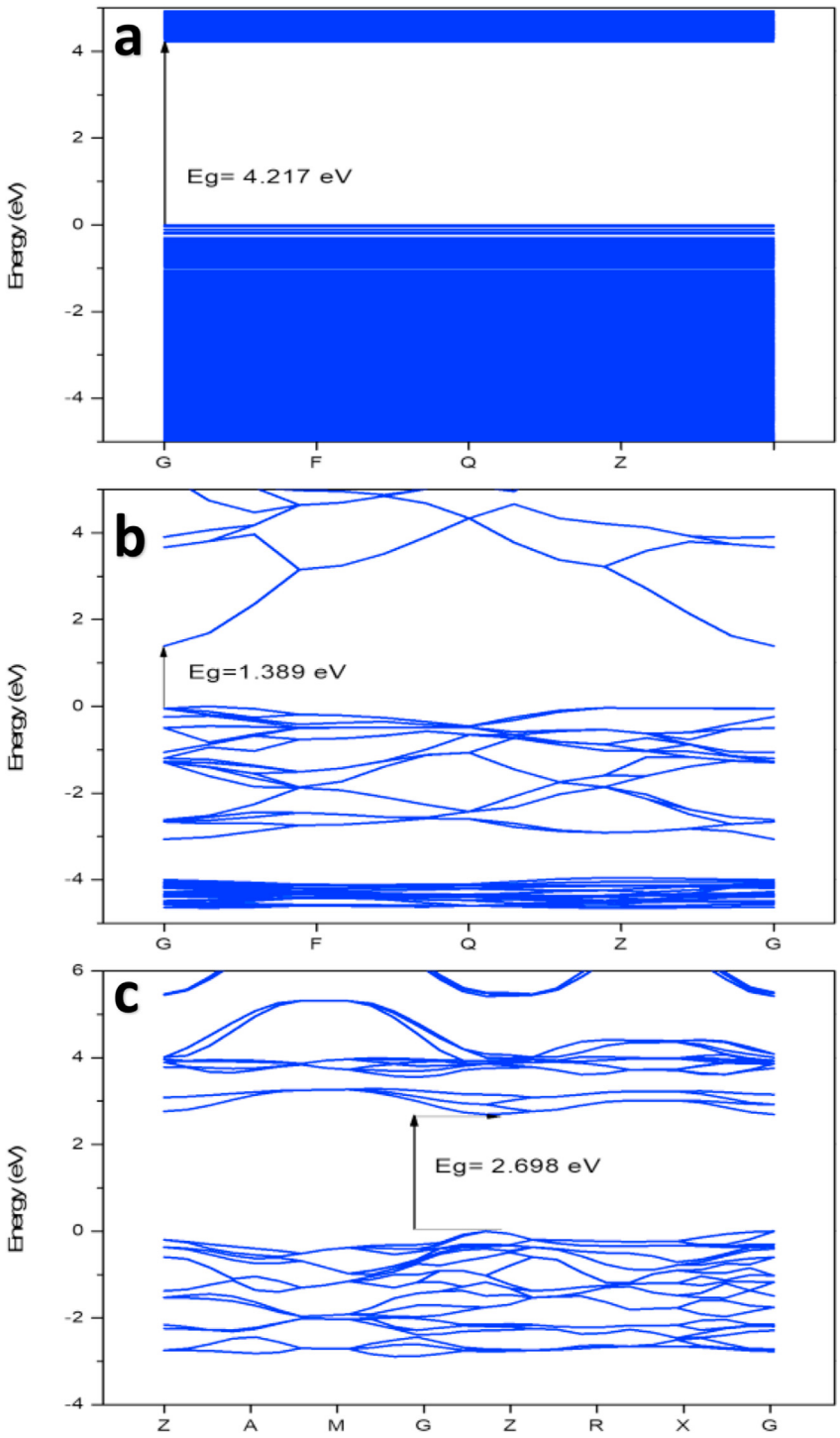

Figure 3. Calculated band structures for (a) rEPS (b) ZnO–ZnS (c)ZnS–ZnO-rEPS.

Table 2. The band gap information for the starting materials and the prepared materials.

Material	Bandgap (eV)	Band type	Conduction band (eV)	Valence band (eV)
rEPS	4.217	Direct	3.852	0.365
ZnO–ZnS	1.389	Direct	1.106	0.283
ZnS–ZnO-rEPS	2.698	Indirect	2.2521	0.4459

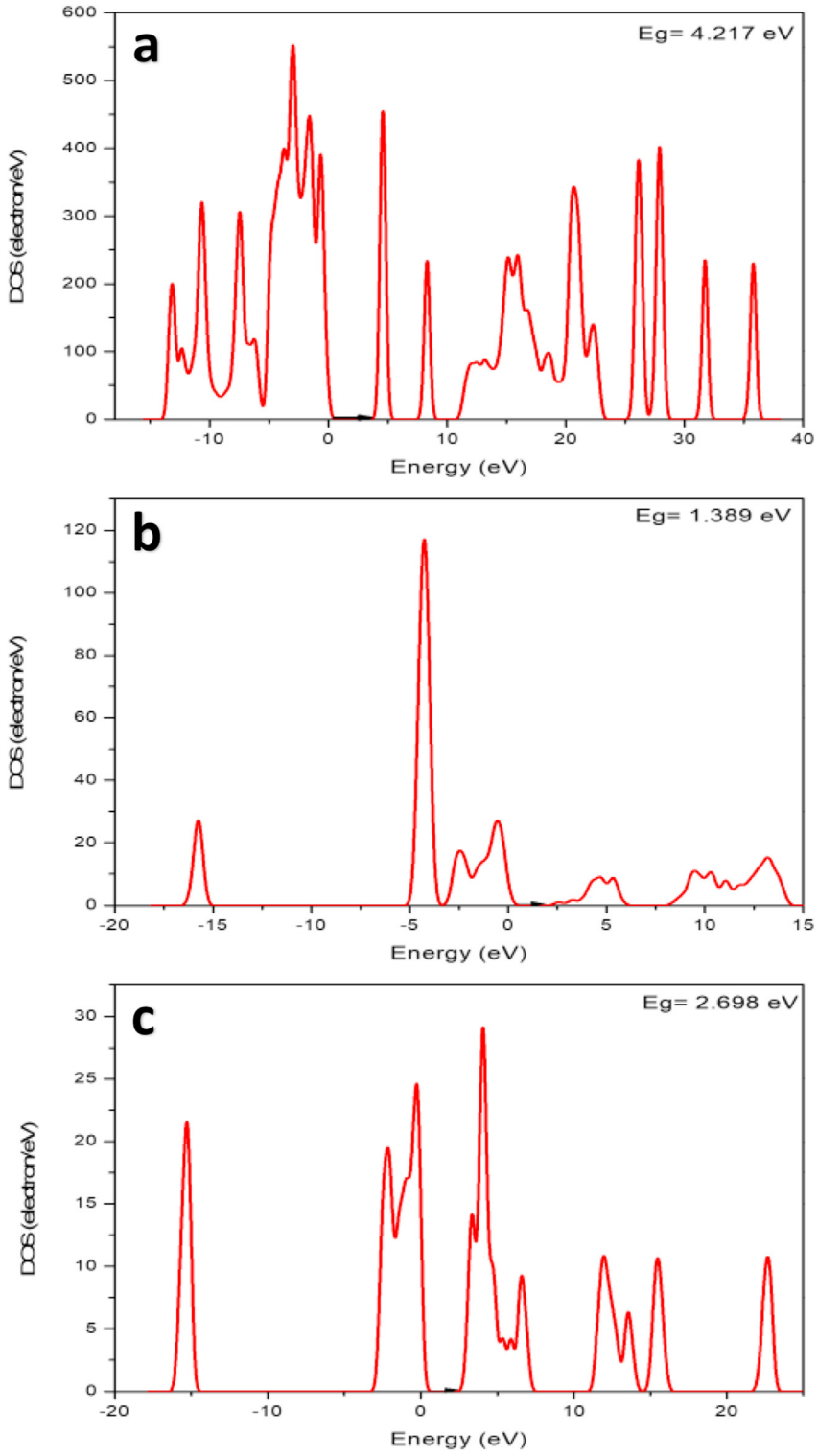

Figure 4. Density of States for (a) rEPS (b) ZnO–ZnS (c)ZnS–ZnO-rEPS.

the ZnS–ZnO sample, and the electronic structure around the VB and CB are very close.

3.3.3. Projected density of states (PDOS)

The projected density of state (PDOS) of the prepared nano-composites samples were plotted to further study the electron distribution and the migration path of the charge carrier (Figure 5). Fermi levels were determined at 0.3937, 0.291 and 0.5708 eV for rEPS, ZnO–ZnS and ZnS–ZnO-rEPS, respectively. However, since the fermi level remains at the VB for the prepared samples, this is indicative of the P-type nature of semiconductors [25]. For the rEPS sample (Figure 5a), the indicated orbitals distributed equally around the fermi level. The

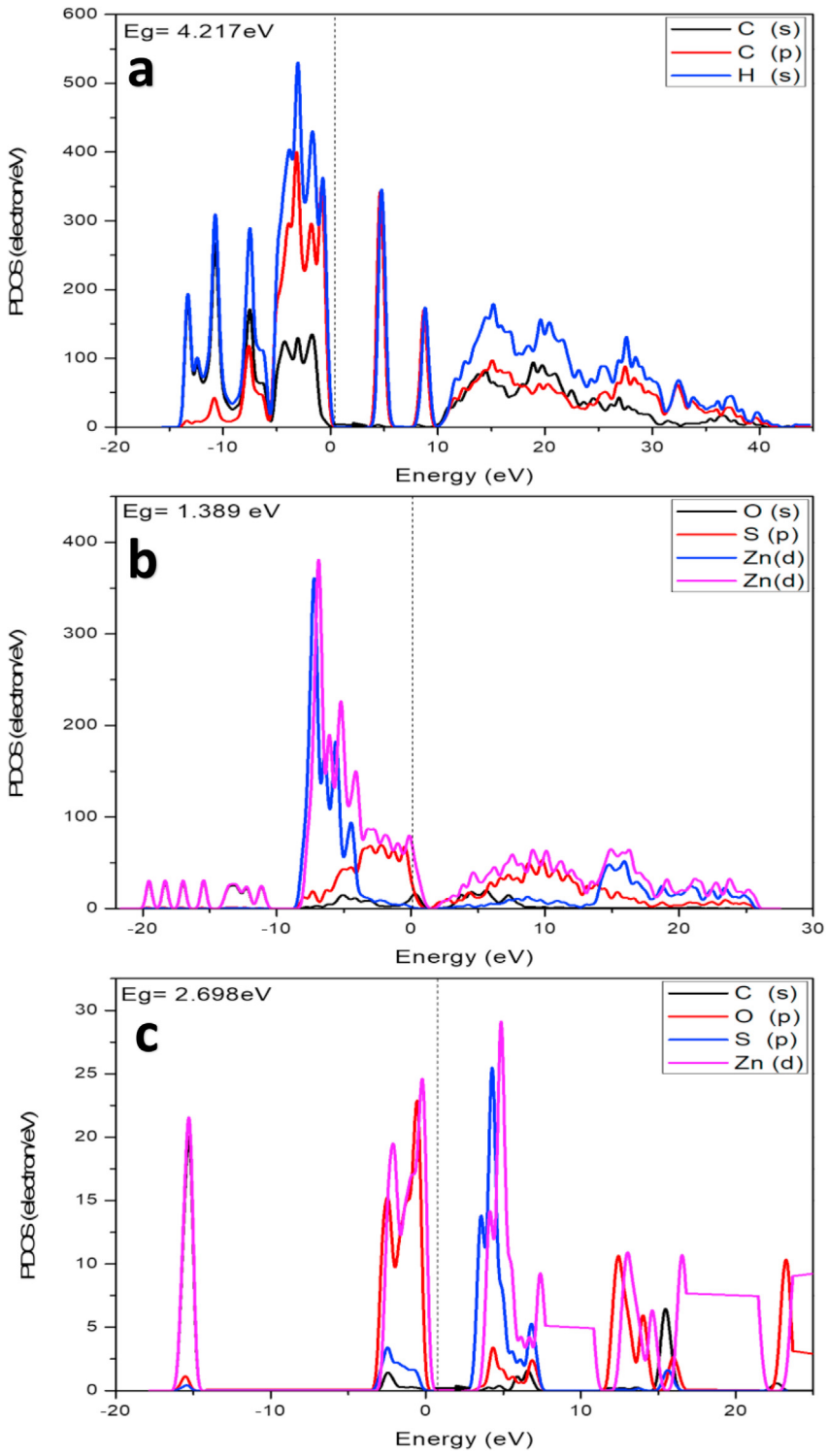

Figure 5. Projected density of states of (a)rEPS, (b)ZnO–ZnS and (c)ZnS–ZnO-rEPS.

Zn-d and S-p electrons, mainly contribute to the electron density for the ZnO–ZnS sample. The O-p and Zn-d orbitals contributes to the conduction and valence bands with lower contribution of O-s. These results are in fair agreement with the experimental findings mentioned in a previous study [26]. Finally, the ZnS–ZnO-rEPS sample shows an interesting PDOS pattern, were all the Zn-d, S-p and O-p orbitals were in both the valence and conduction bands. Although in both the VB and CB the Zn-d orbital had the highest contribution, then the O-p had the second highest contribution to the valence band and S-p was the second highest for conduction band.

4. Conclusions

A rEPS-based nanocomposite was synthesized through a solvothermal method, and a simulation-based study was conducted using the data obtained from the characterization of the synthesized recycled expanded polystyrene (rEPS) nanocomposites. The structural and electronic properties of the prepared samples were obtained using DFT calculations. The band gap of rEPS was found to be 4.217eV, and after combining ZnO and ZnS with rEPS to form a nanocomposite, the bandgap of the ZnS–ZnO-rEPS nanomaterials was 2.698 eV. The calculated bandgap value for the

ZnS–ZnO-rEP nanocomposite indicates the material is a semiconductor that may absorb electromagnetic radiation in the UV-Visible range. It was found that the obtained nanocomposite, ZnO–ZnS-rEPS, is a p-type semiconductor. Most importantly, the calculated band gaps, showed the potential of the ZnO–ZnS-rEPS nanocomposite as a photocatalytic material with activity in the visible region. This also could open up a novel method for recycling of EPS and utilizing it for other applications such as nanoreactors, coating materials, electrochemical biosensors, nanocarriers, and catalysts.

Declarations

Author contribution statement

Rokhsareh Akbarzadeh: Conceived and designed the experiments; Analyzed and interpreted the data; Wrote the paper.

Olusola Olaitan Ayeler: Conceived and designed the experiments; Performed the experiments.

Qusai Ibrahim: Performed the experiments; Analyzed and interpreted the data.

Peter Apata Olubambi: Contributed reagents, materials, analysis tools or data.

Patrick Ndungu: Analyzed and interpreted the data; Contributed reagents, materials, analysis tools or data.

Funding statement

This work was supported by the University of Johannesburg.

Data availability statement

Data will be made available on request.

Declaration of interests statement

The authors declare no conflict of interest.

Additional information

No additional information is available for this paper.

Acknowledgements

Authors appreciate the support of the South African National Research foundation (NRF), the Centre for Nanomaterials Science Research and the Global Excellence Stature (GES) at the University of Johannesburg. The authors would also like to acknowledge the Centre for High Performance Computing (CHPC), South Africa.

References

[1] A. Mishra, A. Mehta, S. Basu, Clay supported TiO_2 nanoparticles for photocatalytic degradation of environmental pollutants: a review, Environ. Chem. Eng. 6 (2018) 6088–6107.

[2] N. Ferronato, V. Torretta, Waste mismanagement in developing countries: a review of global issues, Int. J. Environ. Res. Publ. Health 16 (6) (2019) 1060.

[3] N. Ndugire, et al., Selection, Design and Implementation of Economic Instruments in the Solid Waste Management Sector in Kenya: the Case of Plastic Bags, United Nations Environment Programme, Nairobi, 2005.

[4] P. Violeta Melinte, Lenuta Stroea, L. Andreea, Chibac-scutaru. Polymer nanocomposites for photocatalytic applications, Catalysts 9 (12) (2019) 986.

[5] Ufana Riaz, S.M. Ashraf, Jyoti Kashyap, Role of conducting polymers in enhancing TiO2-based photocatalytic dye degradation: a short review, Polym. Plast. Technol. Eng. 54 (17) (2015) 1850–1870.

[6] T. Krasia-Christoforou, Organic–inorganic polymer hybrids: synthetic strategies and applications, in: Hybrid and Hierarchical Composite Materials, Springer, 2015, pp. 11–63.

[7] M. Oteng-Ababio, Rethinking waste as a resource: insights from a low-income community in Accra, Ghana, City Territ. Architect. 1 (1) (2014) 10.

[8] R.R.N. Bhattacharya, K. Chandrasekhar, P. Roy, A. Khan, Challenges and Opportunities: Plastic Waste Management in India, The Energy and Resources Institute, 2018.

[9] M. Alshabanat, Applications of polystyrene/graphite composites in water purification as a semiconductor visible-light photocatalyst for organic pollutant degradation, Egypt. J. Aquat. Res. 45 (1) (2019) 19–23.

[10] N. Saba, P.M. Tahir, M. Jawaid, A review on potentiality of nano filler/natural fiber filled polymer hybrid composites, Polymers 6 (8) (2014) 2247–2273.

[11] Wei Liu, Bakhtar Ullah, Ching-Ching Kuo, Xingke Cai, Two-dimensional nanomaterials-based polymer composites: fabrication and energy storage applications, Adv. Polym. Technol. (2019). Article ID 4294306, 15 pages.

[12] S. Mallakpour, V. Behranvand, Polymeric nanoparticles: recent development in synthesis and application, Express Polym. Lett. 10 (11) (2016) 895.

[13] Luis Ferney González-Bahamón, Felicien Mazille, Luis Norberto Benítez, César Pulgarín, Photo-Fenton degradation of resorcinol mediated by catalysts based on iron species supported on polymers, J. Photochem. Photobiol. Chem. 217 (Issue 1) (2011) 201–206.

[14] E. Winsberg, Simulated experiments: methodology for a virtual world, Philos. Sci. 70 (1) (2003) 105–125.

[15] O.O. Ayeleru, et al., Nanoindentation studies and characterization of hybrid nanocomposites based on solvothermal process, Inorg. Chem. Commun. (2020) 107704.

[16] H. Search, C. Journals, A. Contact, M. Iopscience, I.P. Address, First-principles Simulation : Ideas , Illustrations and the CASTEP Code, 2002, p. 2717.

[17] J.P. Perdew, K. Burke, M. Ernzerhof, Generalized gradient approximation made simple, Phys. Rev. Lett. 77 (1996) 3865–3868.

[18] C. Adamo, M. Ernzerhof, G.E. Scuseria, C. Adamo, The Meta-GGA Functional: Thermochemistry with a Kinetic Energy Density Dependent Exchange-Correlation Functional the Meta-GGA Functional: Thermochemistry with a Kinetic Energy Density Dependent Exchange-Correlation Functional, 2013, p. 2643 (2000).

[19] Z. Wu, R.E. Cohen, More accurate generalized gradient approximation for solids, Phys. Rev. B Condens. Matter 73 (23) (2006) 2–7.

[20] S. Li, Y.H. Lin, B.P. Zhang, J.F. Li, C.W. Nan, BiFeO 3/TiO 2 core-shell structured nanocomposites as visible-active photocatalysts and their optical response mechanism, J. Appl. Phys. 105 (5) (2009), 054310.

[21] C.B. Ong, L.Y. Ng, A.W. Mohammad, A review of ZnO nanoparticles as solar photocatalysts: synthesis, mechanisms and applications, Renew. Sustain. Energy Rev. 81 (2018) 536–551.

[22] F.K. Shan, Y.S. Yu, Band gap energy of pure and Al-doped ZnO thin films, J. Eur. Ceram. Soc. 24 (6) (2004) 1869–1872.

[23] L. Hu, W. Yi, J. Tang, T. Rao, Z. Ma, C. Hu, T. Li, Planar graphitic ZnS, buckling ZnS monolayers and rolled-up nanotubes as nonlinear optical materials: first-principles simulation, RSC Adv. 9 (44) (2019) 25336–25344.

[24] T. Das, S. Datta, Thermochemical stability, and electronic and dielectric properties of Janus bismuth oxyhalide BiOX (X= Cl, Br, I) monolayers, Nanoscale Adv. 2 (3) (2020) 1090–1104.

[25] H.X. Zhu, J.M. Liu, Electronic structure of organometal halide perovskite CH3 NH3BiI3 and optical absorption extending to infrared region, Sci. Rep. 6 (2016) 37425.

[26] J. Schrier, D.O. Demchenko, A.P. Alivisatos, Optical properties of ZnO/ZnS and ZnO/ZnTe heterostructures for photovoltaic applications, Nano Lett. 7 (8) (2007) 2377–2382.